EXHIBIT C

THE JOURNAL OF BIOLOGICAL CHEMISTRY Vol. 278, No. 23, Issue of June 6, pp. 20812–20820, 2003
© 2003 by The American Society for Biochemistry and Molecular Biology, Inc. Printed in U.S.A.

The Methyl Donor *S*-Adenosylmethionine Inhibits Active Demethylation of DNA

A CANDIDATE NOVEL MECHANISM FOR THE PHARMACOLOGICAL EFFECTS OF *S*-ADENOSYLMETHIONINE*

Received for publication, November 20, 2002, and in revised form, March 25, 2003
Published, JBC Papers in Press, April 3, 2003, DOI 10.1074/jbc.M211813200

Nancy Detich‡§¶, Stefan Hamm§‖, George Just‡‡, J. David Knox‡, and Moshe Szyf‡§§**

*From the Departments of ‡Pharmacology and Therapeutics and **Chemistry, McGill University, Montreal, Quebec H3G 1YG, Canada*

***S*-Adenosylmethionine (AdoMet) is the methyl donor of numerous methylation reactions. The current model is that an increased concentration of AdoMet stimulates DNA methyltransferase reactions, triggering hypermethylation and protecting the genome against global hypomethylation, a hallmark of cancer. Using an assay of active demethylation in HEK 293 cells, we show that AdoMet inhibits active demethylation and expression of an ectopically methylated CMV-GFP (green fluorescent protein) plasmid in a dose-dependent manner. The inhibition of GFP expression is specific to methylated GFP; AdoMet does not inhibit an identical but unmethylated CMV-GFP plasmid. *S*-Adenosylhomocysteine (AdoHcy), the product of methyltransferase reactions utilizing AdoMet does not inhibit demethylation or expression of CMV-GFP. *In vitro*, AdoMet but not AdoHcy inhibits methylated DNA-binding protein 2/DNA demethylase as well as endogenous demethylase activity extracted from HEK 293, suggesting that AdoMet directly inhibits demethylase activity, and that the methyl residue on AdoMet is required for its interaction with demethylase. Taken together, our data support an alternative mechanism of action for AdoMet as an inhibitor of intracellular demethylase activity, which results in hypermethylation of DNA.**

S-Adenosylmethionine (AdoMet)[1] is the main methyl donor in numerous methyltransferase reactions in all organisms (1). The reduced derivative of 5,10-methylenetetrahydrofolate, 5-methyltetrahydrofolate, provides the methyl group for methionine and AdoMet synthesis (2). A series of rodent experiments as well as epidemiological data have suggested a correlation between diets deficient in folate or in sources of methyl groups (*i.e.* foods containing methionine, one-carbon compounds, and choline) and the risk for colorectal adenomas and cancer (3). Such diets, referred to collectively as methyl-deficient, have been shown to promote liver cancer in rodents (4, 5), and AdoMet treatment was shown to prevent the development of liver cancer in rat (6).

In light of the clinical and epidemiological data suggesting a link between AdoMet levels and cancer, it is important to understand the tumor protective mechanism of action of AdoMet, as well as the tumor promoting action of methyl-deficient diets. This is of importance not only for realizing the therapeutic potential of AdoMet, but also for unraveling basic mechanisms of tumorigenesis, especially the role of methyl group metabolism. AdoMet is the cofactor for transmethylation reactions including DNA methylation (7, 8), whereas *S*-adenosylhomocysteine (AdoHcy) is the product of transmethylation reactions and an inhibitor of DNMTs (9). A current model is that exogenous administration of AdoMet increases the intracellular ratio of AdoMet to AdoHcy, thus stimulating DNMT activity resulting in increased DNA methylation (6, 10). An increase in AdoHcy concentrations, even without a concomitant reduction in AdoMet results in inhibition of DNMT and DNA hypomethylation (11). Methyl-deficient diets decrease intracellular AdoMet concentration, increase AdoHcy concentrations, and trigger DNA hypomethylation (5, 12, 13). A genetic link was established between polymorphisms in the *methylenetetrahydrofolate reductase* gene encoding the enzyme catalyzing the synthesis of 5-methyltetrahydrofolate, and DNA hypomethylation (14, 15). Global hypomethylation of DNA is a hallmark of cancer (16, 17). If the mechanism of action of methyl-rich diets in cancer chemoprevention and methyl-deficient diets in cancer promotion is through changing genomic methylation status, then it implies that global hypomethylation plays a causal role in cancer. This hypothesis is supported by the observation that 5-azacytidine, a DNMT inhibitor (18) can reverse AdoMet-mediated chemoprevention of liver carcinogenesis (19).

Although it has been controversial, there is now little doubt (1) that exogenous AdoMet increases the intracellular AdoMet levels. AdoMet uptake into cells has also been verified through a high performance liquid chromatography analysis (20). A number of data support the notion that exogenous AdoMet causes hypermethylation of DNA (10, 21).

Whereas this model provides an attractively simple explanation as to the possible relationship between exogenous AdoMet administration and DNA methylation, there are a number of unresolved issues. First, increased AdoMet should increase DNMT activity only if the normal intracellular concentration of

* This work was supported in part by the National Cancer Institute of Canada and Natural Science and Engineering Research Council Canada. The costs of publication of this article were defrayed in part by the payment of page charges. This article must therefore be hereby marked "*advertisement*" in accordance with 18 U.S.C. Section 1734 solely to indicate this fact.

§ Both authors contributed equally to the results of this work.

¶ Recipient of the Canadian Institute of Health Research Doctoral Fellowship and the McGill Faculty of Medicine Internal Fellowship.

‖ Supported by postdoctoral research stipend from Deutsche Forschungsgemeinschaft.

‡‡ Supported by Grant 228183 from the Natural Science and Engineering Research Council.

§§ To whom correspondence should be addressed: 3655 Sir William Osler Promenade, Montreal, Quebec H3G 1Y6, Canada. Tel.: 514-398-7107; Fax: 514-398-6690; E-mail: mszyf@pharma.mcgill.ca.

[1] The abbreviations used are: AdoMet, *S*-adenosylmethionine; AdoHcy, *S*-adenosylhomocysteine; MBD2, methylated DNA-binding protein 2; dMTase, DNA demethylase; TSA, trichostatin A; DNMT, DNA methyltransferase; GFP, green fluorescent protein.

This paper is available on line at http://www.jbc.org

pressed (RNA and protein) in most hypomethylated tumors (Fig. 3C) is consistent with a mechanism in which a gain of chromosome 15 contributes, at least in part, to the elevated expression of c-*myc*. Moreover, c-*myc* expression was lower in the two tumors that did not show trisomy 15 than in the other tumors (Fig. 3C).

Our results show that genomic hypomethylation causes tumorigenesis in mice and is associated with the acquisition of additional genomic changes. Consistent with this, genomic hypomethylation was found to promote tumorigenesis in a different mouse tumor model and to increase the rate of LOH in cultured fibroblasts (*23*). However, it remains possible that DNA hypomethylation contributes to tumorigenesis through other mechanisms unrelated to chromosomal instability. The phenotype of hypomethylated mice is also consistent with that of *Suv39h* histone methyltransferase mutant mice; hence, DNA and histone methylation, pericentric chromatin structure, and the maintenance of chromosomal stability may be linked (*30*).

DNA methyltransferase inhibitors such as 5-aza-2′-deoxycytidine have been used successfully to treat cancer in humans (*19, 31*) and mice (*32, 33*). The efficacy of these drugs is presumably due to their ability to reverse the epigenetic silencing of tumor suppressor genes. In light of our results, however, this therapeutic strategy should perhaps be considered a double-edged sword: Genomic demethylation may protect against some cancers such as intestinal tumors in the Apc^{Min} mouse model (*32*) but may promote genomic instability and LOH (*20, 23*) and increase the risk of cancer in other tissues, as seen in hypomethylated mutant mice.

References and Notes

1. P. A. Jones, S. B. Baylin, *Nature Rev. Genet.* **3**, 415 (2002).
2. A. P. Feinberg, B. Vogelstein, *Nature* **301**, 89 (1983).
3. M. Ehrlich, *Oncogene* **21**, 5400 (2002).
4. M. A. Gama-Sosa, *Nucleic Acids Res.* **11**, 6883 (1983).
5. J. N. Lapeyre, F. F. Becker, *Biochem. Biophys. Res. Commun.* **87**, 698 (1979).
6. R. Jaenisch, A. Bird, *Nature Genet.* **33** (suppl.), 245 (2003).
7. H. Lei *et al.*, *Development* **122**, 3195 (1996).
8. E. Li, T. H. Bestor, R. Jaenisch, *Cell* **69**, 915 (1992).
9. K. L. Tucker *et al.*, *Genes Dev.* **10**, 1008 (1996).
10. C. P. Walsh, J. R. Chaillet, T. H. Bestor, *Nature Genet.* **20**, 116 (1998).
11. F. Gaudet, A. Eden, R. Jaenisch, unpublished data.
12. S. Cory, D. L. Vaux, A. Strasser, A. W. Harris, J. M. Adams, *Cancer Res.* **59** (suppl.), 1685s (1999).
13. R. Jaenisch, A. Schnieke, K. Harbers, *Proc. Natl. Acad. Sci. U.S.A.* **82**, 1451 (1985).
14. R. Jaenisch, *Proc. Natl. Acad. Sci. U.S.A.* **73**, 1260 (1976).
15. D. Jahner, R. Jaenisch, *Nature* **287**, 456 (1980).
16. L. Jackson-Grusby *et al.*, *Nature Genet.* **27**, 31 (2001).
17. G. Selten, H. T. Cuypers, M. Zijlstra, C. Melief, A. Berns, *EMBO J.* **3**, 3215 (1984).
18. E. Wainfan, L. A. Poirier, *Cancer Res.* **52**, 2071s (1992).
19. A. R. Karpf, D. A. Jones, *Oncogene* **21**, 5496 (2002).
20. R. Z. Chen, U. Pettersson, C. Beard, L. Jackson-Grusby, R. Jaenisch, *Nature* **395**, 89 (1998).
21. C. Lengauer, K. W. Kinzler, B. Vogelstein, *Proc. Natl. Acad. Sci. U.S.A.* **94**, 2545 (1997).
22. B. N. Trinh, T. I. Long, A. E. Nickel, D. Shibata, P. W. Laird, *Mol. Cell. Biol.* **22**, 2906 (2002).
23. A. Eden, F. Gaudet, A. Waghmare, R. Jaenisch, *Science* **300**, 455 (2003).
24. M. Jeanpierre *et al.*, *Hum. Mol. Genet.* **2**, 731 (1993).
25. G. L. Xu *et al.*, *Nature* **402**, 187 (1999).
26. G. Hodgson *et al.*, *Nature Genet.* **29**, 459 (2001).
27. C. Stewart, K. Harbers, D. Jahner, R. Jaenisch, *Science* **221**, 760 (1983).
28. Z. Wirschubsky, P. Tsichlis, G. Klein, J. Sumegi, *Int. J. Cancer* **38**, 739 (1986).
29. M. Muto, Y. Chen, E. Kubo, K. Mita, *Jpn. J. Cancer Res.* **87**, 247 (1996).
30. A. H. F. M. Peters *et al.*, *Cell* **107**, 323 (2001).
31. V. Zagonel *et al.*, *Leukemia* **7** (suppl. 1), 30 (1993).
32. P. W. Laird *et al.*, *Cell* **81**, 197 (1995).
33. A. R. MacLeod, M. Szyf, *J. Biol. Chem.* **270**, 8037 (1995).
34. F. Gaudet, D. Talbot, H. Leonhardt, R. Jaenisch, *J. Biol. Chem.* **273**, 32725 (1998).
35. C. E. Whitehurst, S. Chattopadhyay, J. Chen, *Immunity* **10**, 313 (1999).

36. We thank R. Flannery for help with the mouse colony, and K. Hong and C. Cardoso for helpful discussions. Supported by grants from the Max Delbrück Center and the Deutsche Forschungsgemeinschaft (H.L.), by NIH grant CA87869 (R.J.), and by EMBO fellowship ALTF 43-1999 and Boehringer Ingelheim (A.E.).

18 February 2003; accepted 10 March 2003

PAGE 30/50 * RCVD AT 10/18/2004 1:17:29 PM [Eastern Daylight Time] * SVR:USPTO-EFXRF-1/1 * DNIS:8729306 * CSID:4256410880 * DURATION (mm-ss):70-04

(i) Hypomethylation may induce endogenous retroviral elements, leading in turn to insertional activation of proto-oncogenes (*13*). To test this idea, we hybridized RNA from randomly selected tumors with a Moloney murine leukemia virus (MMLV) cDNA probe and an IAP probe to detect endogenous retroviral and IAP expression, respectively. Of nine *Dnmt1*$^{chip/-}$ tumors, none showed C-type retroviral activation (Fig. 3A) (*14*) and only one of eight tumors showed a moderate increase in IAP expression (Fig. 3B, lane 7). In contrast, strong C-type retroviral expression was seen in a MMLV-induced lymphoma [Fig. 3A, slot a1 (*15*)] and IAP expression was highly activated in *Dnmt1*$^{-/-}$ fibroblasts [Fig. 3B, lanes 10 to 12 (*16*)]. Because c-*myc* is a frequent target for insertional activation by retroviral elements (*17*), we searched for inserted proviral elements in hypomethylated and MMLV-induced tumors. In 3 of 12 MMLV-induced tumors, an insertional rearrangement was seen in the vicinity of the c-*myc* locus, in agreement with previous observations (*17*). In contrast, no rearrangements were detected in hypomethylated tumors [0/18 (*11*)]. We conclude that the extent of hypomethylation in *Dnmt1*$^{chip/-}$ mice does not effectively activate endogenous retroviral elements and that virus insertions may not be a prevalent mechanism in hypomethylation-induced lymphoma.

(ii) Hypomethylation may activate proto-oncogenes through epigenetic effects (*18, 19*). Indeed, c-*myc* was overexpressed in most hypomethylated tumors (Fig. 3C). However, it is unlikely that activation of c-*myc* is a direct consequence of promoter demethylation because the gene is expressed at normal levels in thymuses from 2- and 4-week-old mice that show a level of hypomethylation identical to that of the tumors [Fig. 1D (*11*)]. In addition, c-*myc* was not activated in *Dnmt*$^{-/-}$ fibroblasts that are almost completely demethylated (*16*). Finally, if oncogene activation by hypomethylation stimulated T cell proliferation as a first step in transformation, one would expect the lymphomas to be polyclonal rather than monoclonal (Fig. 2C).

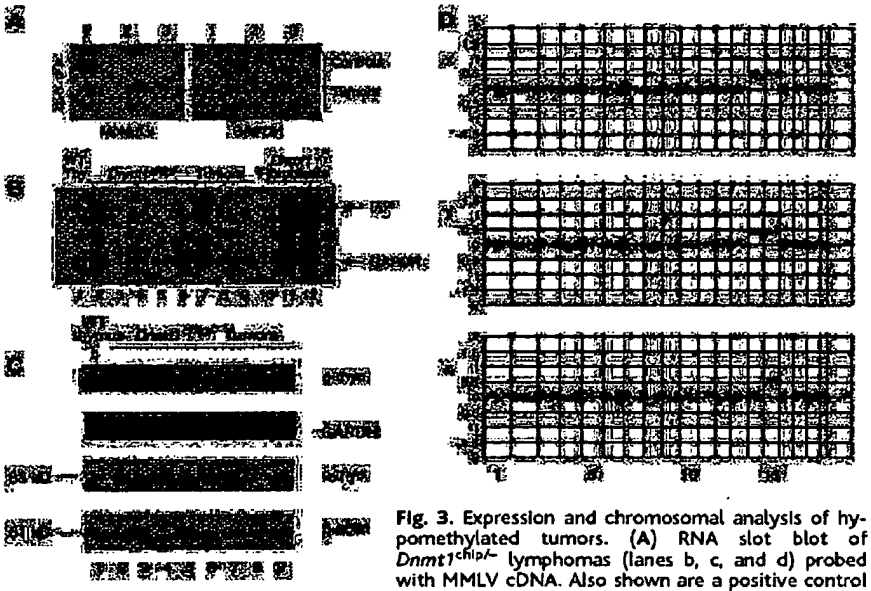

Fig. 3. Expression and chromosomal analysis of hypomethylated tumors. (**A**) RNA slot blot of *Dnmt1*$^{chip/-}$ lymphomas (lanes b, c, and d) probed with MMLV cDNA. Also shown are a positive control lymphoma from a Mov-1 mouse [slot a1 (*15*)] and negative control thymuses from wild-type 129/Sv (slot a2) and a wild-type littermate of a tumor-bearing mouse (slot a3). (**B**) Northern blot of IAPs in *Dnmt1*$^{chip/-}$ tumors. IAPs can be detected in most tumors, whereas wild-type thymus does not show IAP expression. Positive control (lanes 10 to 12, 1:3 serial dilutions) are *Dnmt1*$^{-/-}$ hypomethylated fibroblasts that have been shown to activate IAP expression (*16*). Comparison of IAP and glyceraldehyde-3-phosphate dehydrogenase (GAPDH) levels shows that most clones express much less IAPs than the positive control. (**C**) Expression levels of c-*myc* were assessed by Northern blot (top two panels) and by immunoblot (bottom two panels). Lanes 2 to 7 are tumors that showed chromosome 15 trisomy; lanes 8 and 9 are tumors that are diploid for chromosome 15. Probes used were c-*myc* exon 2 for the Northern analysis and a rabbit polyclonal IgG antibody to c-*myc* for immunoblots (Santa Cruz Biotechnology). (**D**) Array comparative genome hybridization (CGH) analyses of three *Dnmt1*$^{chip/-}$ tumors, showing clear single-copy, whole-chromosome gain of chromosome 15 (x, y, and z), whole-chromosome gains of 14 and loss on distal 12 (x), and gains of chromosome 14 and proximal 9 (y). The X gain (x) reflects a sex difference between tumor and control. Array CGH was performed as in (*26*). Fluorescence ratios (average of quadruplicate measurements) for each bacterial artificial chromosome are plotted as a function of genome location based on the February 2002 freeze of the assembled mouse genome sequence (http://genome.ucsc.edu). Vertical lines delimit chromosome boundaries.

(iii) Hypomethylation may induce genomic instability. In fact, a significantly increased frequency of chromosomal rearrangements such as loss of heterozygosity (LOH) was observed in *Dnmt1* mutant ES cells, suggesting that normal levels of methylation are important for genomic stability (*20*). Defects in DNA methylation have been linked to genome instability in studies of colorectal tumor cell lines (*21*), mouse tumor models (*22, 23*), and patients with immunodeficiency–centromeric instability–facial anomalies (ICF) syndrome (*24, 25*).

To test whether DNA hypomethylation increases genomic instability in *Dnmt1*$^{chip/-}$ tumors, we performed array-based comparative genome hybridization [array CGH (*26*)] using thymic tumor genomic DNA prepared from *Dnmt1*$^{chip/-}$ and Mov-1 (*15*) and Mov-14 (*27*) MMLV transgenic mice (Fig. 3D). There was a statistically significant difference in chromosome gains between these tumor classes (Table 1). Ten of 12 hypomethylated tumors exhibited a gain of chromosome 15, whereas only 2 of 12 MMLV-induced tumors showed this change ($P = 0.004$). Relative to MMLV-induced tumors, hypomethylated tumors also displayed a gain of chromosome 14 (4/12 versus 0/12, $P = 0.05$) and a higher degree of duplicated and deleted chromosome regions (Table 1) (Fig. 3D).

Together with the centromeric hypomethylation we observed (Fig. 1C), these results suggest a causal link between DNA hypomethylation and chromosomal instability as one mechanism leading to tumorigenesis. The increased fluorescence ratios observed for chromosomes 14 and 15 are consistent with single-copy whole-chromosome gains throughout the tumor (Fig. 3D), which suggests that they are early events in the development of these monoclonal T cell lymphomas. Chromosome 15 is frequently duplicated in mouse T cell tumors (*28, 29*) and contains the oncogene c-*myc*, which when overexpressed causes T cell lymphomas (*17*). The fact that c-*myc* is overex-

Table 1. Gains or losses of chromosomes in *Dnmt1*$^{chip/-}$ and MMLV-induced tumors. The numbers indicate the number of times a particular event occurred in the *Dnmt1*$^{chip/-}$ or Moloney tumors. These events were not mutually exclusive; many tumors exhibited multiple chromosomal events.

Chromosomal changes	*Dnmt1*$^{chip/-}$ tumors ($n = 12$)	MMLV-induced tumors ($n = 12$)
Chr 15 gain	10	2
Chr 14 gain	4	0
Chr 10 gain	0	1
Partial Chr 9 gain	2	0
Partial Chr 4 gain	1	0
Partial Chr 16 loss	1	0
Partial Chr 12 loss	1	0

PAGE 31/50 * RCVD AT 10/18/2004 1:17:29 PM [Eastern Daylight Time] * SVR:USPTO-EFXRF-1/1 * DNIS:8729306 * CSID:4256410880 * DURATION (mm-ss):70-04

ation. *Dnmt1*$^{chip/-}$ embryonic stem (ES) cells expressed 10% of wild-type levels (Fig. 1A). To test whether the reduced Dnmt1 expression affected DNA methylation in vivo, we generated mice carrying the different *Dnmt1* alleles and determined their global methylation levels with the use of a probe for endogenous retroviral A type particles (IAPs) (Fig. 1, B and D) (*10*) and centromeric repeats (Fig. 1C). Southern blot analysis of embryonic fibroblasts and adult tissues showed that the DNA from compound heterozygotes was hypomethylated relative to the DNA from *Dnmt1*$^{chip/chip}$ or *Dnmt1*$^{+/+}$ mice, although substantially less so than the DNA from *Dnmt1*$^{-/-}$ null ES cells. Mice carrying the different *Dnmt1* alleles were obtained at the expected Mendelian ratios, indicating that reduction of Dnmt1 expression to 10% was compatible with viability. However, compound heterozygotes (*Dnmt1*$^{chip/-}$) were runted and their weight at birth was only 70% that of *Dnmt1*$^{+/-}$ mice, in contrast to mice homozygous for the hypomorphic allele (*Dnmt1*$^{chip/chip}$), which were normal in size (Fig. 2A). *Dnmt1*$^{chip/-}$ mice, although remaining substantially underweight, were fertile and generated litters of nonrunted pups when bred with wild-type mice.

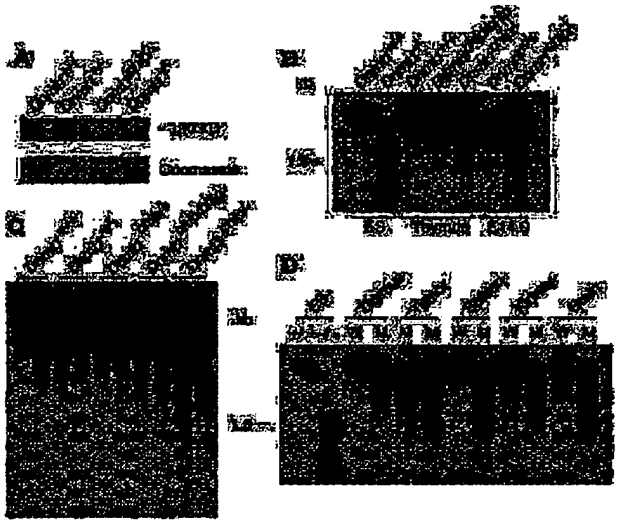

Fig. 1. Genomic hypomethylation in *Dnmt1* hypomorphic mice. (A) Immunoblot analysis of protein extracts from ES cells, using a C-terminal Dnmt1 chicken antibody (*34*). The level of Dnmt1 in *Dnmt1*$^{chip/-}$ ES cells was markedly reduced, demonstrating the hypomorphic nature of this allele. The *Dnmt1*$^{-/-}$ negative control extracts did not show any bands, as expected [c allele (*7*)]. A Promega antibody to chicken immunoglobulin Y (IgY), with horseradish peroxidase as secondary antibody, was used; detection was performed with the Amersham Pharmacia Biotech ECL kit. The Coomassie gel shows total protein levels in each sample. (B) Southern blot of methylation status of IAPs in *Dnmt1*$^{chip/chip}$ and *Dnmt1*$^{chip/-}$ mice. Genomic DNA was digested with the methylation-sensitive restriction enzyme Hpa II and probed with an IAP cDNA probe (*10*). Hypomethylation was detected in thymus from 6-week-old *Dnmt1*$^{chip/-}$ mice and in *Dnmt1*$^{chip/-}$ embryonic day (E) 14.0 fibroblasts but not in *Dnmt1*$^{chip/chip}$ homozygotes or wild-type controls, as evidenced by the presence of lower molecular weight DNA fragments. (C) Southern blot analysis of centromeric repeat methylation of E14.0 fibroblasts from mice containing various *Dnmt1* alleles. Hypomethylation is evident in the *Dnmt1*$^{chip/-}$ lanes. (D) Southern blot analysis of IAP methylation status in tissues from a 6-week-old *Dnmt1*$^{chip/-}$ mouse and in lymphomas. Significant hypomethylation is evident in all *Dnmt1*$^{chip/-}$ tissues. Controls for methylation (*Dnmt1*$^{+/+}$ ES cells) and hypomethylation (*Dnmt1*$^{-/-}$ ES cells) are also shown (ES, ES cells; W, *Dnmt1*$^{+/+}$; M, *Dnmt1*$^{chip/-}$).

In addition to the runted phenotype, 80% of *Dnmt1*$^{chip/-}$ mice developed aggressive thymic tumors at 4 to 8 months of age. Cumulative survival of the *Dnmt1*$^{chip/-}$ mice is shown in Fig. 2B. Histological analysis classified the tumors as T cell lymphomas (*11*), and fluorescence-activated cell sorting (FACS) analysis revealed that most tumors were CD4$^-$/CD8$^+$ or CD4$^+$/CD8$^+$ (Fig. 2D). When tested for D-to-J rearrangements in the T cell receptor β locus, four of 10 tumors showed a predominant Dβ1-to-Jβ1 rearranged band (Fig. 2C, lanes 5, 9, 11, and 13) consistent with monoclonality. Tumors without Dβ1-to-Jβ1 recombination may have rearranged other D and J elements. Monoclonality suggests that hypomethylation induces cancer in a precursor cell, with subsequent events leading to malignant tumor formation. Consistent with frequent activation of the c-*myc* oncogene in mouse and human lymphoma (*12*), we found that c-*myc* was overexpressed in almost all hypomethylated tumors (15/18 *Dnmt1*$^{chip/-}$, Fig. 3C).

Genomic hypomethylation may contribute to lymphomagenesis by an epigenetic or a genetic mechanism. We considered three possible mechanisms.

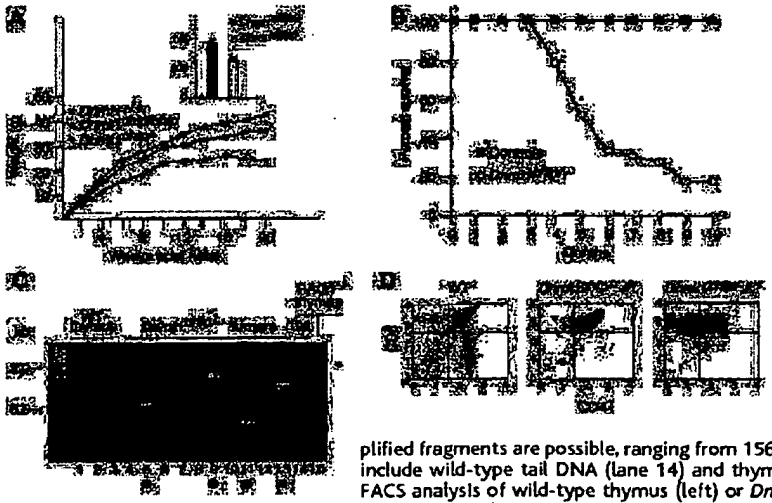

Fig. 2. *Dnmt1* hypomorphs are runted and develop T cell lymphomas. (A) Average weight of *Dnmt1*$^{chip/+}$ (n = 20) and *Dnmt1*$^{chip/-}$ (n = 20) male littermates at birth (Inset). *Dnmt1*$^{chip/-}$ mice were 66% as large as *Dnmt1*$^{chip/+}$ mice. Females showed the same runt phenotype. The error bar indicates ±1 SD, $p < 0.0001$ (Student t test, StatView 5.0.1 software). Also shown are growth curves of *Dnmt1*$^{chip/chip}$, *Dnmt1*$^{chip/-}$, and wild-type male mice. Six to 10 mice of each genotype were used for each data point. (B) Cumulative survival of *Dnmt1*$^{chip/-}$ mice. Most *Dnmt1*$^{chip/-}$ mice became terminally ill between 4 and 8 months of age. Control mice were *Dnmt1*$^{chip/chip}$ (n = 18); experimental mice were *Dnmt1*$^{chip/-}$ (n = 33). Mice were autopsied when visibly ill. At autopsy, 23 of 33 *Dnmt1*$^{chip/-}$ mice had developed tumors (21 lymphomas and 2 fibrosarcomas). Autopsy of *Dnmt1*$^{chip/chip}$ mice at 6 months (n = 12) and 12 months (n = 6) showed no evidence of tumor formation. (C) Dβ1-to-Jβ1 rearrangement at the TCRβ locus was analyzed by the polymerase chain reaction as described (*35*), using primers 1 and 4 therein. The asterisk denotes the germline configuration [2171 base pairs (bp)]. When rearranged, five different amplified fragments are possible, ranging from 1561 to 381 bp (see wild-type thymus, lanes 1 to 3). Controls also include wild-type tail DNA (lane 14) and thymus DNA from a recombination-deficient RAG1$^{-/-}$ mouse. (D) FACS analysis of wild-type thymus (left) or *Dnmt1*$^{chip/-}$ tumors (middle and right) stained for CD4 and CD8 receptors, T cell–specific markers. Tumors analyzed (n = 16) contained either double-positive CD4^{high}/CD8^{high} cells (9/16, middle panel) or CD4^{low}/CD8^{high} cells (7/16, right panel).

PAGE 32/50 * RCVD AT 10/18/2004 1:17:29 PM [Eastern Daylight Time] * SVR:USPTO-EFXRF-1/1 * DNIS:8729306 * CSID:4256410880 * DURATION (mm-ss):70-04